ResearchGate

See discussions, stats, and author profiles for this publication at: https://www.researchgate.net/publication/51735636

Electron microscopy of specimens in liquid. Nat. Nanotechnol. 6, 695–704

Article *in* Nature Nanotechnology · November 2011

DOI: 10.1038/nnano.2011.161 · Source: PubMed

CITATIONS
181

READS
396

2 authors, including:

Niels De Jonge
INM - Leibniz Institute for New Materials
137 PUBLICATIONS **2,529** CITATIONS

SEE PROFILE

All in-text references underlined in blue are linked to publications on ResearchGate, letting you access and read them immediately.

Available from: Niels De Jonge
Retrieved on: 18 September 2016

nature nanotechnology

REVIEW ARTICLE

PUBLISHED ONLINE: 23 OCTOBER 2011 | DOI: 10.1038/NNANO.2011.161

Electron microscopy of specimens in liquid

Niels de Jonge[1]* and Frances M. Ross[2]*

Imaging samples in liquids with electron microscopy can provide unique insights into biological systems, such as cells containing labelled proteins, and into processes of importance in materials science, such as nanoparticle synthesis and electrochemical deposition. Here we review recent progress in the use of electron microscopy in liquids and its applications. We examine the experimental challenges involved and the resolution that can be achieved with different forms of the technique. We conclude by assessing the potential role that electron microscopy of liquid samples can play in areas such as energy storage and bioimaging.

Liquid-phase processes are important over a wide range of areas in science and technology, including biological activity in cells, biomineralization, the low-cost synthesis of nanoparticles and electrochemical reactions for energy storage. Electron microscopy opens a unique window into structures and processes in the liquid phase, as it provides a combination of temporal and spatial resolution that is not achievable with other techniques. Transmission electron microscopy (TEM) of samples in liquid has a history stretching back as far as the earliest electron microscopes[1]. But, over the past decade, electron microscopy of liquid samples has experienced a surge of interest, generated by advances in thin-film[2] and microchip technology[3]. Recent applications have included the imaging of labelled structures within whole cells[4], electrochemical reactions[3,5] and solution-phase nanoparticle growth[6]. In this review, we discuss the experimental basis of liquid electron microscopy, comparing the different approaches that have been used to solve the fundamental problem of the technique — the incompatibility of a liquid sample with the vacuum environment needed for electron microscopy. We describe recent applications in biology and materials science, and quantify the spatial resolution that can be expected within liquids imaged in different electron microscopy modalities. We also consider the present experimental limitations, particularly electron beam effects, and conclude with an outlook on future experimental developments for electron microscopy in liquids and its application in new scientific fields.

Strategies for electron microscopy of samples in liquids

The three commonly used types of electron microscope each generate images via different contrast mechanisms[7–9]. In TEM, a stationary, spread electron beam with energy between ~60 and 300 keV irradiates a sample that is thinner (often much thinner) than 0.5 μm. The sample modifies the phase and amplitude of the transmitted electrons, so that the resulting image contains information about the sample. In scanning TEM (STEM), the image is recorded by scanning a focused beam over the sample and detecting transmitted electrons pixel by pixel. Scanning electron microscopy (SEM) scans a focused beam, typically with energy between ~500 eV and 30 keV, over the surface of a (bulk) sample, collecting backscattered or secondary electrons pixel by pixel. All electron microscopes require a vacuum, both to allow operation of the electron source and to minimize scattering other than from the sample. Samples must therefore be stable under vacuum, and so are traditionally prepared in the solid state.

However, ever since the invention of the electron microscope, a goal has been to image liquid samples as easily as with a light microscope, but with much higher spatial resolution[1,10]. Liquids that have low vapour pressure[5] or that are already encapsulated by another material[11] can be examined without special precautions. But, the majority of liquid samples, including those involving water, require other strategies. The earliest system[1] consisted of an open environmental chamber in the sample region of a TEM (Fig. 1a). Using differential pumping, this chamber could be kept at a pressure up to 0.2 bar to create a wet sample environment containing both liquid and vapour, while the rest of the microscope remained at low pressure[12].

Open environmental chambers are now used in modern *in situ* TEMs for both gas- and liquid-phase reactions[13,14]. However, it is difficult to control the liquid thickness accurately in an open environmental chamber, making it challenging to obtain liquid films thinner than ~1 μm, as required for nanometre-scale resolution in TEM. Instead, it proved more practical to develop the environmental chamber for imaging liquids in SEM[15], where there is of course no requirement for a thin sample. Environmental SEM, or ESEM (Fig. 1b), is now widely used to image the surface of samples in a vapour environment, achieving a spatial resolution in the nanometre range[16,17].

The open environmental chamber is not suitable if, for example, the sample must be embedded in a liquid layer of controlled thickness, or if the experiment requires a flowing liquid. The problem then becomes that of designing a thin yet stable liquid layer. This is achieved by means of a hermetically sealed enclosure, or 'liquid cell', that constrains the liquid into a layer less than a few micrometres thick. In the first decades of electron microscopy, various systems were developed that used electron-transparent membranes to create such closed liquid cells (Fig. 1c)[12,18]. However, the liquid layers were still not particularly thin, and the spatial resolution achieved[12] was often not much better than what was available, with much less effort, through light microscopy.

Over the past decade, developments in thin-film technology, microfabrication and imaging have brought new life to the use of liquid cells[3]. Thin carbon foils[19,20] and graphene sheets[21] have been used as membranes, but thin (20–100 nm) SiN films supported on silicon microchips are increasingly popular, as they are easily manufactured, homogeneous in composition and thickness, and make robust windows for liquid cells with designs such as those shown in Fig. 2a–d,g. Standard silicon processing techniques allow electrodes to be integrated onto the microchips[3,22], increasing the

[1]Department of Molecular Physiology and Biophysics, Vanderbilt University School of Medicine, 2215 Garland Avenue, Nashville, Tennessee 37232, USA, [2]IBM T. J. Watson Research Center, 1101 Kitchawan Road, Yorktown Heights, New York 10598, USA. *e-mail: niels.de.jonge@vanderbilt.edu; fmross@us.ibm.com

© 2011 Macmillan Publishers Limited. All rights reserved

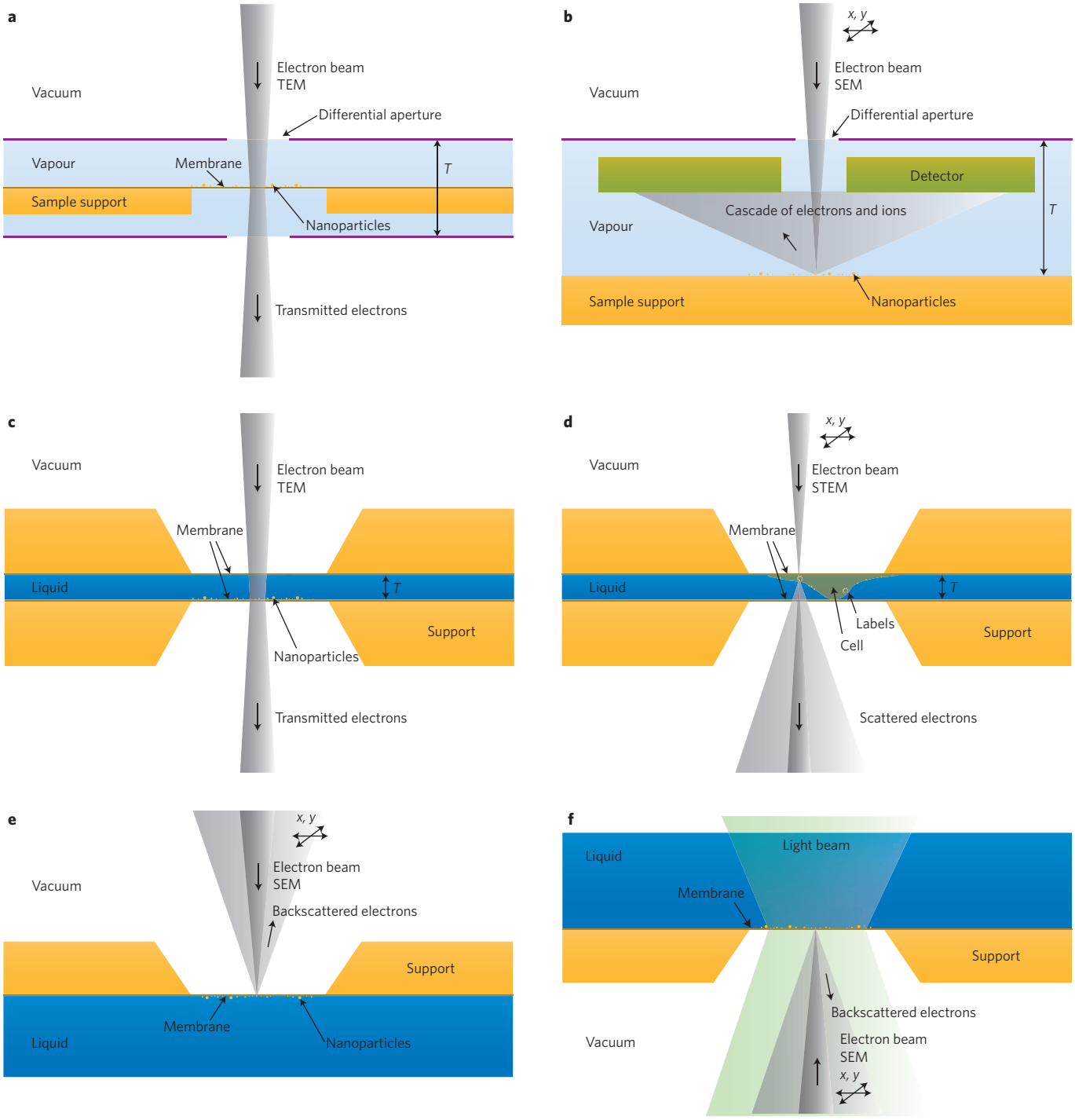

Figure 1 | Configurations for electron microscopy in liquid. a, TEM imaging with an open environmental chamber containing liquid and vapour. Differential apertures separate the microscope vacuum from the higher pressure at the sample. **b**, SEM imaging with an environmental chamber. The electron beam scans in *x* and *y* directions over the sample. **c**, TEM imaging of nanoparticles in a liquid fully enclosed between electron transparent windows. **d**, STEM imaging in a fully enclosed liquid, used to image nanoparticle labels on whole biological cells. **e**, SEM of a liquid sample under an electron transparent window. **f**, Combination of SEM and light microscopy of a liquid sample above an electron transparent window.

range of experiments possible. Careful design has simplified assembly[22–24], and can even permit the use of flowing liquids[4,25], as in Fig. 2c,d. Finally, imaging can be optimized, using STEM to obtain nanometre-scale resolution even through several micrometres of water[4,26] (Fig. 1d).

These advances have paved the way for liquid TEM and STEM to make a significant impact in biological and materials science. Of course, experimental difficulties still remain. One issue particular to experiments involving liquid cells is balancing window size, liquid thickness and window thickness with field of view and image resolution. Resolution improves as the liquid layer and windows become thinner, as we show below. However, thin windows bow under vacuum, increasing the liquid thickness in the centre of the window[27]. To optimize resolution, one may consider connecting the windows

© 2011 Macmillan Publishers Limited. All rights reserved

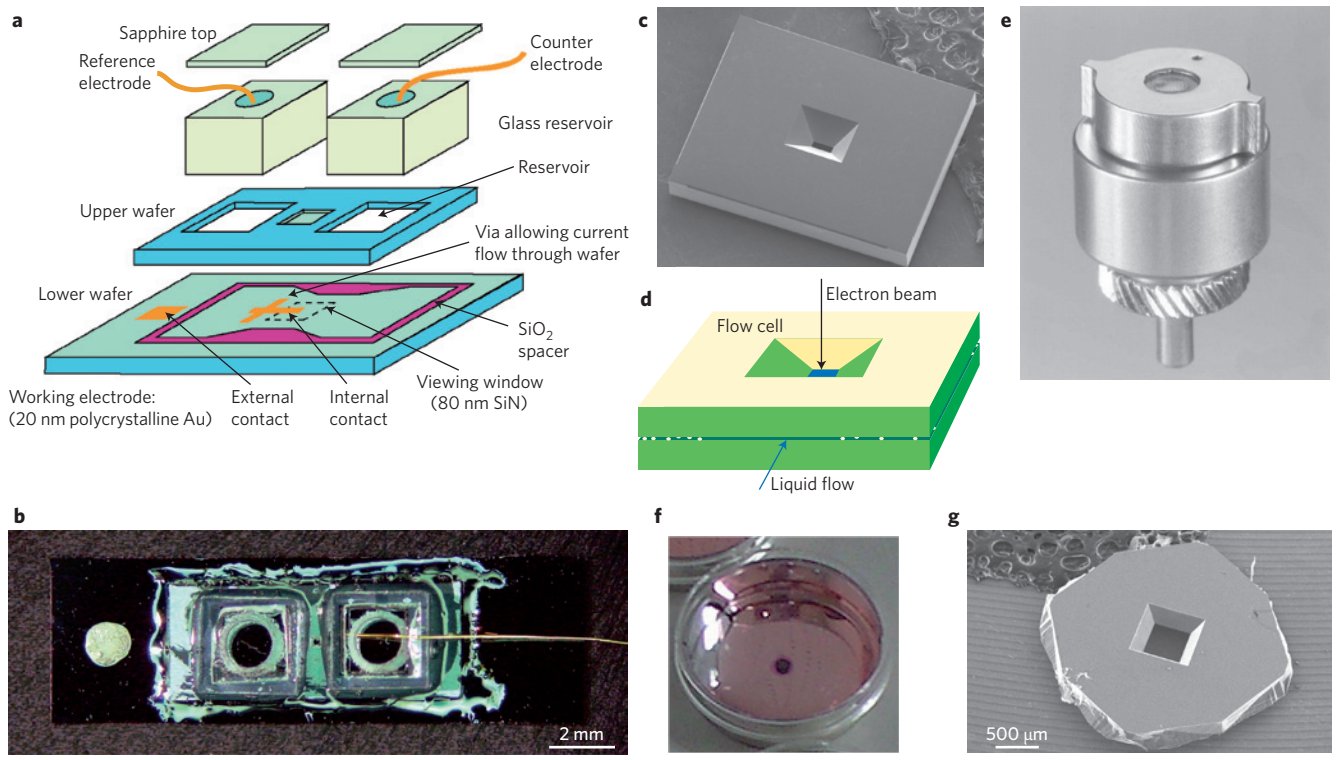

Figure 2 | Examples of electron microscopy systems for liquids. a, Fabrication of a liquid cell from Si microchips (upper and lower wafers) with SiN windows, glass reservoirs, lids and three electrodes for electrochemical TEM experiments[3]. **b**, Photograph of an assembled liquid cell. **c**, A single Si microchip with an electron transparent SiN window[25]. The dimensions of the microchip are 2.0 × 2.3 × 0.3 mm. **d**, A microfluidic chamber formed from two of the microchips in **c**, showing the liquid flow direction. **e**, A capsule with an electron transparent window for imaging liquid samples in SEM[43]. The outer diameter is 16 mm. **f**, Cell culture dish with a microchip with a SiN window[33], for combined light microscopy and SEM. **g**, The back (vacuum) side of the microchip for the culture dish. Panels reproduced with permission from: **a**,**b**, ref. 3, © 2003 NPG; **c**, ref. 25, © 2010 CUP; **e**, ref. 43, © 2004 Informa Healthcare; **f**,**g**, ref. 33, © 2010 Elsevier. Panel **d** modified with permission from ref. 4, © 2009 National Academy of Sciences.

by pillars[28–30], or using wafer bonding[22] to reduce window separation. The window thickness itself may limit the resolution; this can sometimes be overcome by using graphene sheets to enclose the sample[21]. The formation of bubbles in the liquid layer[27,31] also causes problems. Uncontrolled bubble formation may be alleviated by flowing the liquid[25], although the reduced liquid thickness at a bubble actually improves resolution[27,32].

Thin window systems are useful in SEM as well as in TEM and STEM. A closed liquid cell, similar to those used in TEM, allows transmitted signals in the SEM to be collected[22]. Alternatively, a 'capsule' with a single window can enable SEM of samples fully immersed in liquid by collecting a backscattered signal through the window[2] (Figs 1e and 2e). Backscatter imaging through a window is advantageous in that it allows SEM to be combined with light microscopy[33] (Fig. 1f). A liquid sample in a dish with an integrated window (Fig. 2f,g) can be imaged with light microscopy from the liquid side or SEM from the window side[33]. This approach allows correlative microscopy as well as possibilities such as excitation of fluorescent materials with the electron beam at nanometre localization[34].

It may at first appear counterintuitive, but excellent spatial resolution is possible in liquid layers, down to a few nanometres even through several micrometres of liquid[4,26], or atomic resolution for very thin water layers[35]. Temporal resolution can also be good, so dynamic processes can be observed[3,6,35]. However, electron beam effects provide a practical limitation. After discussing applications in biological and materials science, we will therefore consider the opportunities and limitations of electron microscopy in liquids in terms of resolution and beam effects.

Applications in the life sciences

A central challenge in modern biological research is the visualization of the molecular machinery underlying cellular function[36]. This requires innovative microscopy techniques capable of studying the constituents of cells, many of which are smaller than the wavelength of light. State-of-the-art cryo electron microscopy preserves cellular structures by converting cellular water into amorphous ice via the preparation of cryo sections[37,38]. However, the cells are no longer intact or in their native liquid state, and high concentrations of amorphous ice-inducing solutes are often used, which may induce changes in the biological system. There is thus a pressing need for nanoscale microscopy of cells and other biological systems and materials in the liquid state.

Open environmental chambers have been extensively studied for biological imaging, and ESEM[17] can image the surfaces of pristine cells in a wet environment. The cells must first be transferred to a cooled pure-water environment[39]. Various microorganisms withstand transfer to pure water, and ESEM provides images of their pristine surfaces[40]. However, for eukaryotic cells this transfer process alters cellular morphology owing to changes in osmotic pressure. Better images of eukaryotic cells are obtained from fixed, but still hydrated samples[39] (Fig. 3a). Including a STEM detector in the ESEM can allow imaging of the intracellular structure[41].

To preserve cells in as pristine a state as possible, they should be fully surrounded by saline. Figure 3b shows a backscatter SEM image, recorded in a liquid capsule (Fig. 2e), of surface receptors labelled with 20-nm-diameter Au nanoparticles on a fixed *Helicobacter pylori* bacterium[2]. Some particles display sharp contours, whereas others appear blurred; presumably these are at

© 2011 Macmillan Publishers Limited. All rights reserved

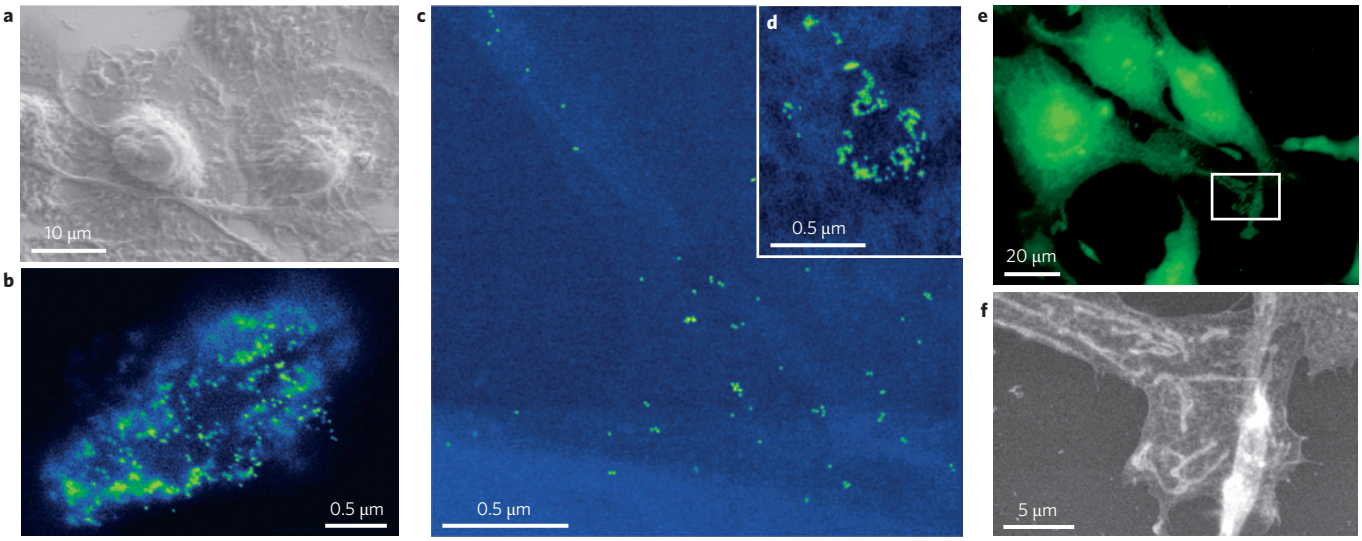

Figure 3 | Electron microscopy of biological samples. a, Human monocyte-derived macrophages imaged with SEM in a wet environment[39] at 4.9 torr and 7 °C. Samples were fixed in glutaraldehyde and rinsed with deionized water before imaging. **b**, SEM image of *H. pylori* bacterium fully immersed in liquid, imaged using a capsule with a thin window. Samples were incubated with complexed biotinylated gastrin on streptavidin-coated 20 nm Au particles, followed by glutaraldehyde fixation. **c**, STEM image of Au-labelled epidermal growth factor receptors on whole fixed COS7 fibroblast cells in liquid. The Au labels are visible as yellow spots on the light blue cellular material. The background shows in dark blue. **d**, Endocytotic vesicles were formed in a second sample after a longer incubation. **e**, Fluorescence microscopy image of COS7 cells[33]. The cells were fixed, labelled with a fluorescent dye, and stained for contrast in SEM. **f**, SEM image of the cellular material in the rectangle in **e** imaged under fully hydrated conditions[33]. Panels reproduced with permission from: **a**, ref. 39, © 2009 Wiley; **e**,**f**, ref. 33, © 2010 Elsevier. Panels modified with permission from: **b**, ref. 2, © 2004 National Academy of Sciences; **c**,**d**, ref. 4, © 2009 National Academy of Sciences.

different depths in the liquid. This high-quality imaging of Au nanoparticles in water is an exciting development, as well-established techniques already allow specific proteins to be labelled with Au nanoparticles[42]. The liquid capsule can also be used to visualize tissue in fully hydrated conditions after fixation and staining to enhance the SEM contrast[43]. The liquid capsule is particularly advantageous for questions involving lipid membranes in cells, as these are difficult to preserve during dehydration and washing steps[44]. Another benefit is that sample preparation and visualization is rapid.

In TEM, environmental chambers[12,19,45] and closed liquid cells[24] have both been used for biological imaging, although with limited success in competing with the resolution of light microscopy, except when using diffraction techniques[46]. Instead, as we discuss below, STEM[4,25–27] provides dramatically improved resolution of Au-labelled structures in the several-micrometres-thick liquid layers needed to enclose eukaryotic cells. This is illustrated in Fig. 3c, where Au-labelled epidermal growth factor (EGF) molecules bound to cellular EGF receptors of whole fixed fibroblast cells were imaged with STEM[4] at a spatial resolution (on the labels) of 4 nm, using a microfluidic chamber[25] (Fig. 2c,d) filled with saline. The capability for studying biological function is illustrated in Fig. 3d, where cells were incubated with labelled EGF until endocytosis occurred; the Au nanoparticles are organized into a round shape, interpreted as an endocytotic vesicle inside the cell. It is worth noting that no radiation damage effects were observed on the spatial distribution of the labels for the dose used, 7×10^4 electrons per nm^2. Other microscopy methodologies cannot resolve the positions of labelled proteins on intact cells with such high resolution[47]. First results have also been reported on the imaging of eukaryotic cells that were kept alive in a microfluidic device and then imaged with STEM to study nanoparticle uptake[48] and to investigate the pristine ultrastructure of yeast mutants[49].

The combination of electron microscopy with regular cell culture handling and light microscopy is particularly useful in biological investigations[33] (Fig. 2g,h). Standard cell biology experiments can be performed on electron transparent membranes, with the cells imaged with light microscopy (Fig. 3e) and then with SEM after fixation and staining if needed (Fig. 3f). By imaging multiple cells, the interfacing of neurons[33] or the effect of cholesterol depletion on microdomain organization in tumour cells[50] can be studied. The correlative approach has also been demonstrated for fluorescence microscopy and STEM, to study the locations of receptors specifically labelled with quantum dots[51], and to image yeast cells[49].

Applications in materials science

Materials science applications benefit from both the spatial resolution available with liquid cell electron microscopy and its temporal resolution, which allows reaction kinetics and mechanisms to be probed. Electrochemical processes provide an excellent example, with observations possible in a liquid cell that is filled with an electrolyte and also contains electrodes. In Fig. 2a, three electrodes in a TEM liquid cell are connected externally to a potentiostat[3,52]; for SEM imaging, electrodes can be readily incorporated on microchips[33]. Figure 4a shows a series of images obtained during electrodeposition of Cu onto an electron-transparent Au electrode patterned over one of the windows of a TEM liquid cell[52]. Nucleation and growth of individual Cu clusters is well resolved, with simultaneous measurement of voltage and current. Growth is reversible and can be repeated on the same area under different conditions. By measuring individual clusters rather than ensemble properties, such experiments probe the textbook understanding of electrochemical growth. In Fig. 4a, diffusion-limited growth models[53] cannot explain the nucleation density and growth rates observed; the modifications required to these growth models[52] have implications for the control of electrodeposited morphology. Nucleation sites, cluster correlations and growth exponents are also accessible by liquid cell TEM[3,54,55].

A practical advantage of electrochemical reactions is that they can be initiated when the liquid cell is ready for imaging in the

© 2011 Macmillan Publishers Limited. All rights reserved

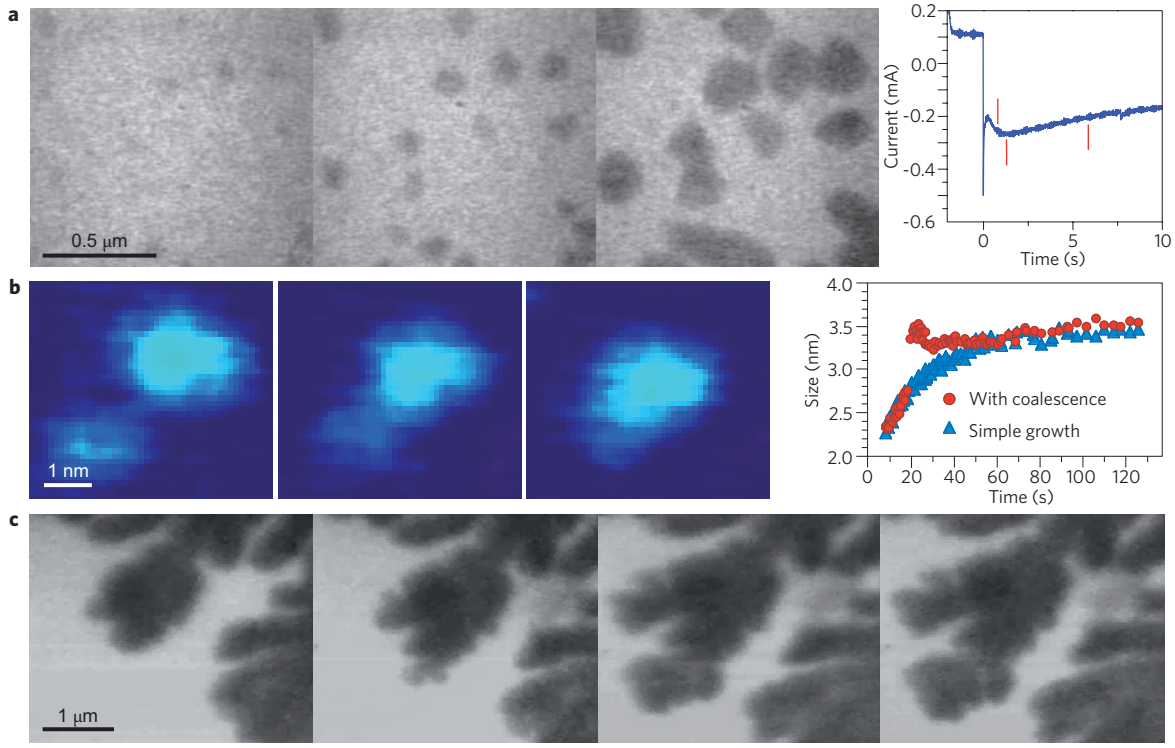

Figure 4 | Liquid cell electron microscopy in materials science. a, Images and electrochemical data obtained during potentiostatic deposition of Cu on a polycrystalline Au electrode from 0.1M $CuSO_4$/0.18M H_2SO_4. Cu has dark contrast whereas the Au (20 nm thick), SiN windows (80 nm thick) and electrolyte (1 μm thick) provide the grey background. The applied potential was −70 mV with respect to a Cu reference electrode, and the graph shows the total current versus time. The electrode area is 2×10^{-5} cm^2. Red lines show the times of each image. **b**, Images acquired during Pt nanoparticle formation from a solution containing 10 mg mL^{-1} Pt(acetylacetonate)$_2$ in a 9:1 mixture of *o*-dichlorobenzene and oleylamine. The images were recorded after 17.9, 18.7, and 22.3 s of beam exposure during which a coalescence event occurs. The graph shows the size of this (red circles) and another particle that appears to grow by addition of monomers (blue triangles). **c**, Energy filtered images at 16 s intervals during dendritic growth of Cu from the edge of an electrode[6]. Galvanostatic conditions were used with current density 40 mA cm^{-2} and average lateral growth rate 0.2 μm s^{-1}. Panels modified with permission from: **a**, ref. 52, © 2006 ACS; **b**, ref. 6, © 2009 AAAS; **c**, ref. 104, © 2010 CUP.

microscope. Spontaneously occurring processes can be more challenging as they may start to take place while setting up the liquid cell. Some experiments therefore make use of slow evaporation of the liquid through an imperfect seal, perhaps accelerated by the electron beam[32]. Diffusion of individual particles in liquids is visible[20,23,25,29] and, when examined during slow evaporation, allows testing of Brownian motion theories[32]. Alternatively, the beam itself may stimulate a process through heating or non-thermal effects. For example, beam-induced platinum nanoparticle formation in a Pt^+-containing solution (Fig. 4b) demonstrates two coexisting mechanisms, growth by coalescence and growth by addition of monomers[6], and PbS nanoparticles can form either under the beam or by light stimulation[35]. Understanding the size distribution of solution-phase nanoparticles is important for developing the particles for applications, and individual measurements can suggest detailed growth models.

Once nanoparticles have formed, a key question is how they assemble into flat or three-dimensional arrangements, and how this self-assembly can be controlled. Beam-induced assembly of particles has been observed by liquid cell SEM[22], whereas the dispersion of nanoparticles in solution has been quantified in liquid cell TEM[23], measuring the degree of dispersion without the artefacts caused by drying a solution and doing conventional TEM analysis.

The differentially pumped open environmental chamber allows examination of reactions where less precise liquid-thickness control is required. An example from atmospheric science is the hygroscopic behaviour of inorganic atmospheric particles[56]. Other applications include catalytic reactions involving liquids, such as the sequence used to form nylon[57], liquid-phase synthesis of nanoparticles[58] and nanoparticle self-assembly at liquid interfaces[14].

Finally, even a standard TEM without an environmental chamber or liquid cell allows examination of encapsulated and low-vapour-pressure liquids. Encapsulated liquids include, for example, liquid inclusions of Pb formed by implantation into an Al matrix, whose solidification kinetics can be examined via TEM heating experiments[59], and liquid Xe in Al, where ordering at the liquid/solid interface can be measured[11]. Many low-vapour-pressure liquids participate in interesting growth processes and phase transformations. For example, liquid AuSi droplets catalyse Si nanowire growth, observable directly in the TEM[60] because of the low vapour pressure of AuSi (10^{-10} torr) at the growth temperature. Similarly, phase transformations, surface reactions and growth processes can be measured in metal alloy droplets[61–63]. Ionic liquids also have low enough vapour pressure for direct observation in SEM[64,65] or TEM[5]. This allows for the interesting possibility of passing current through the liquid and thereby modelling reactions relevant to battery science. By placing a droplet of a Li-containing ionic liquid on a carbon electrode, contacting it with a SnO_2 nanowire, and applying a voltage, lithiation of the nanowire was observed with TEM[5], taking place via a sequence of microstructural changes that included dislocation formation and amorphization. This experiment suggests broad opportunities for liquid-based electron microscopy studies relevant to energy storage.

© 2011 Macmillan Publishers Limited. All rights reserved

The resolution of electron microscopy in liquids

To use the full potential of electron microscopy of liquids it is important to understand the ultimate performance possible, the major experimental limitations, and how these compare with other techniques. In the following sections we therefore consider the resolution expected for imaging in liquids, based on the fundamental equations describing the interactions of an electron beam with matter, and discuss the effects of beam–sample interactions on resolution.

The resolution in TEM. For TEM, the highest resolution for an object within a liquid is achieved when the object is at the electron beam exit side of the sample (Fig. 1c). To a first approximation, the window material itself can be considered transparent for typical beam energies. Instead, the resolution-limiting factor is chromatic aberration caused by inelastic scattering of electrons by the liquid[31]. The full-width at half-maximum of the energy distribution ΔE of transmitted electrons follows from calculations of the inelastic electron scattering cross-section and is given by the following equation[8]:

$$\Delta E = \frac{N_A e^4 Z \rho T}{2\pi\varepsilon_0^2 W m_0^2 v^2} \quad (1)$$

Here, N_A is Avogadro's number, e is the elementary charge, Z the atomic number, ρ the density and T the thickness of the liquid layer, ε_0 the permittivity of space, W the atomic weight, m_0 the mass and v the velocity of the electrons. This energy broadening affects the resolution of the image because of the chromatic aberration of the objective lens. The image resolution d_c can be approximated by[8]:

$$d_c = \alpha C_c \frac{\Delta E}{2E} \quad (2)$$

where α is the objective semi-angle, C_c is the chromatic aberration coefficient and E is the beam energy. For water, where[26,66] $Z = 4.7$, we can combine equations (1) and (2) into the following expression for the resolution:

$$d_{TEM} = 6\times10^{12} \frac{\alpha C_c T}{E^2} \quad (3)$$

with E in eV (using ρ in g m^{-3} in equation (2)). For typical values, α = 10 mrad, C_c = 2 mm, E = 200 keV and T = 1 μm, we obtain d_{TEM} = 4 nm, consistent with experimental findings[31]. (At 300 keV, a higher d_{TEM} of ~1 nm has been obtained in organic solvent[6].) Figure 5 shows the resolution as function of the liquid thickness for 200 keV and the above microscope settings.

Equation (3) gives the best possible resolution; worse resolution will be seen for objects positioned further from the exit side of the sample, as elastic scattering of electrons in the liquid between the focal plane and the window will broaden the beam[26,67–70]. For example, a TEM image of a particle at the top of a 1-μm-thick water layer would have a resolution of only ~12 nm. However, it is worth noting that diffraction techniques can be used in TEM when the sample in liquid contains repetitive units[12], and this may allow higher resolution information to be obtained.

The resolution in STEM. For STEM, the highest resolution for an object within a liquid is achieved when the object is at the entrance side of the sample (Fig. 1d)[4,71]. The image is formed pixel by pixel by scanning a focused electron probe over the sample, and contrast is commonly obtained by using an annular dark-field detector to collect electrons that are elastically scattered out of the primary electron beam. Unlike TEM, nanometre resolution has been obtained in STEM, even for micrometres-thick samples[26,67,72,73]. The fraction N/N_0 of electrons detected, that is, scattered by an angle larger than the opening semi-angle of the detector β, is[8]:

$$\frac{N}{N_0} = 1-\exp\left(-\frac{T}{l}\right), l = \frac{W}{\sigma(\beta)\rho N_A} \quad (4)$$

Here, l is the mean free path length for elastic scattering and $\sigma(\beta)$ is the partial cross section for elastic scattering. The elastic scattering, and hence the image contrast in STEM, is highly sensitive[74,75] to W, ρ and Z (so-called Z-contrast) via $\sigma(\beta)$, making STEM extremely effective for imaging heavy nanoparticles in a light liquid. For example[4,26], with β = 70 mrad and E = 200 keV, we obtain l_{gold} = 73 nm and l_{water} = 10.5 μm. The STEM resolution in a liquid sample can be thought of as the diameter of the smallest nanoparticle visible above the background noise[4,26]:

$$d_{STEM} = 5l_{nanoparticle}\sqrt{\frac{T}{N_0 l_{liquid}}} \quad (5)$$

According to this equation, a 1.4-nm-diameter Au nanoparticle can be resolved on a water layer[26] of T = 5 μm, using a probe current of 0.5 nA and a pixel dwell time of 10 μs. Figure 5 includes the STEM resolution as function of T for these microscope settings, matching experimental data[26,35]. For nanoparticles positioned deeper in the liquid, imaging takes place with a blurred probe, but a resolution better than 10 nm is still achieved in the top 1 μm layer of the liquid[26].

The resolution in SEM. In SEM of enclosed liquid samples, contrast is generated via backscattering of electrons in the sample after passing through the window[8] (Fig. 1e). However, because of the low beam energy used in SEM compared with TEM, the electron probe is already considerably broadened by the time it reaches the liquid. The resolution follows from the beam broadening equation[76]:

$$d_{SEM} \cong 6.1\times10^3 T^{3/2}\frac{Z}{E}\left(\frac{\rho}{W}\right)^{1/2} \quad (6)$$

where T, Z, ρ and W are parameters of the membrane. Note that for SEM the beam broadening is calculated on the basis of the diameter containing 90% of the current[76], accounting for the large interaction volume of the electron beam with the sample, whereas smaller measures are used for (S)TEM[8,26,67]. For a typical SiN window 30 nm thick[33], the beam size, and hence best SEM resolution, calculated from equation (6) is 7 nm at 20 keV (Fig. 5). This is consistent with experimental findings[33] of ~8 nm.

The resolution does not depend on the total liquid thickness, of course, but it does decrease rapidly for nanoparticles deeper in the liquid. For example, at a depth of 100 nm, the resolution is already reduced to 20 nm. SEM should thus be used to study structures in close proximity to the window. The window thickness is also of crucial importance. A system using a ~150 nm thick plastic window provided maximal ~20 nm resolution for Au nanoparticles[2,77]. For ESEM, the resolution can approach that of SEM in vacuum, but as the liquid layer on the sample surface increases in thickness, the resolution also drops dramatically.

Radiation damage. Electron beam–sample interactions are a key factor in any electron microscopy experiment. For liquid samples, a rigorous interpretation of results certainly requires an understanding of beam effects. This can be complicated by the variety of possible interactions and the need for quantitative models for beam–liquid interactions.

© 2011 Macmillan Publishers Limited. All rights reserved

The materials science investigations described above have considered a variety of thermal and non-thermal beam effects. Beam heating is calculated[29] to result in only a small temperature rise (a few degrees or less) because of the good thermal conductivity of the thick liquid cell samples. Beam heating may nevertheless alter diffusion and reaction rates through convection, while even a slight temperature rise alters electrochemical kinetics. Non-thermal effects may be more important and are more complicated, depending on the system under study. High-energy electrons in water produce relatively long-lived species such as OH radicals and hydrated electrons[78,79]. These species may be key to electron-beam-induced formation of nanoparticles from solvated species[6,80]. Solution chemistry is then important — for example, charged species in solution may quench the radicals and reduce their reactivity[78] — but substrate chemistry is also important, as reactive species can also be generated from beam–substrate interactions[65]. The charged species may also influence the currents measured in an electrochemical experiment. Clearly, experiments under different conditions of accelerating voltage or beam intensity are necessary to evaluate the effect of the beam on any liquid-phase phenomenon under study.

Organic samples are known to be strongly affected by relatively small electron doses. For pristine biological material, structural damage starts to occur at the subnanometre scale[81] at ~10^2 electrons per nm^2. This threshold dose is a factor of ten lower than the dose limit for cryo TEM[38]. Fortunately, the dose typically scales quadratically with the resolution[71], and in many cases the experiment can be designed such that a useful resolution can still be obtained within the limit of radiation damage. Recording, for instance, a 1024 × 1024 pixel TEM image of a 1-μm-thick sample with 20 nm resolution would require a 10 nm pixel size and an integration time of ~0.2 s for a typical beam current of 10 nA. The resulting dose of 1.2×10^2 electrons per nm^2 is within the limit of radiation damage. Staying below the threshold dose permitted STEM imaging of yeast cells with a resolution[49] of ~30 nm, and TEM recording of protein crystal diffraction patterns containing subnanometre information[12]. Above the threshold, a better image resolution (a few nanometres) may still be possible, as the overall structure will remain in place at least for some time after damage at the subnanometre scale occurs (for example, by breaking of chemical bonds). If a much higher dose is required, the sample would have to be stabilized by fixation, allowing doses[4] of ~7×10^4 electrons per nm^2. Another approach to overcome radiation damage is to use high contrast nanoparticle labels in combination with STEM imaging. Equations (1)–(6) suggest that 4 nm resolution on a Au nanoparticle in 1 μm of water requires only 1.2×10^2 electrons per nm^2. A larger dose is probably allowed as some structural damage can be tolerated before the locations of the labels change too much. Compared with TEM and STEM, SEM is unfavourable in terms of radiation dose, because the entire beam energy is typically deposited in the sample.

Temporal resolution. Typical image acquisition rates (time resolution) are over 10 frames per second for TEM, whereas the dwell time needed to form each pixel in a STEM or SEM image is typically in the range of 1–60 μs. Although this makes electron microscopy of liquids excellent for studying time-dependent phenomena, as described above, it is worth noting that Brownian motion may limit the achievable image resolution, particularly when imaging live cells or other structures not fixed to the walls of the liquid chamber. Membrane proteins, for example, exhibit diffusion constants[82] as high as 1 μm^2 s^{-1} under physiological conditions, which may lead to movement of several nanometres within the typical pixel time of STEM. The achievable spatial resolution will thus be influenced by parameters such as viscosity, diffusion constants, image acquisition time and also the distance from the window[83].

Even given the limitations on resolution due to Brownian motion and beam effects, the combination of spatial and temporal resolution

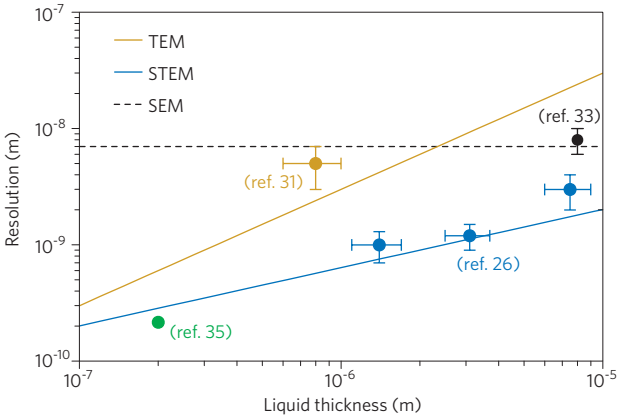

Figure 5 | Resolution of different forms of electron microscopy in liquid. Theoretical maximal resolution versus water thickness for TEM, STEM and SEM. The resolution was calculated for typical TEM and STEM instrument parameters at 200 keV beam energy (see text), and for the imaging of Au nanoparticles at the bottom of a layer of water for TEM, and at the top of the layer for STEM. The resolution obtained in SEM just below the liquid-enclosing membrane does not depend on the liquid thickness (see text). Experimental data points are shown for Au nanoparticles in TEM[31], STEM[26] and SEM with a 30-nm-thick SiN window[33], and for PbS nanoparticles in water imaged with STEM[35]. The error bars represent experimental errors.

of electron microscopy in liquids is unique. Standard light microscopy is limited by diffraction to a spatial resolution[84] of ~200 nm. Super-resolution light microscopy[47,85,86] achieves 20–30 nm resolution, but requires dedicated fluorescent labels, and is limited in temporal resolution for the higher spatial resolution. X-ray microscopy has a resolution in the tens of nanometres range[87,88]. Scanning probe microscopy exhibits nanometre resolution in liquids, but video-rate image acquisition is optimized for flat surfaces (for example, refs 89–92). Any given problem is best addressed by multiple techniques; liquid cell electron microscopy should be able to provide key information for many scientific questions.

Outlook

Electron microscopy in liquids offers a combination of nanoscale spatial resolution and subsecond temporal resolution that suggests significant potential in numerous scientific and technological areas. We anticipate that improvements in experimental capabilities and advances in the quantification of results will lead to application in a wider future range of scientific problems.

In terms of experimental advances, the recent improvements in aberration correction that are revolutionizing the TEM and STEM community[75] will certainly also impact electron microscopy in liquids[35]. Equation (3) showed that the resolution of TEM in liquids is limited by chromatic aberration, in other words, by imperfect focusing of electrons that have different energies. Preventing electrons from contributing to the image if they have lost more than a certain amount of energy would therefore improve the resolution. Such energy filtering allows[93], in principle, subnanometre spatial resolution for liquid layers with a thickness well above 0.5 μm for TEM. However, energy filtering also increases the required dose for imaging. Instead, correction of the chromatic aberration in the electron lenses[94] should improve the resolution in a more dose-efficient way. Temporal resolution should also see a significant improvement. Imaging with speeds of several tens of milliseconds per frame is possible with modern detectors, and in addition, ultrafast TEM has emerged, which uses pulses of electrons triggered by an incident laser beam[95,96]. The short imaging times require high beam currents to obtain sufficient signal-to-noise, giving rise to Coulomb

© 2011 Macmillan Publishers Limited. All rights reserved

interactions that reduce the effective brightness of the electron beam, and thus the achievable spatial resolution[97]. The capability to image materials in liquid using pulses of electrons potentially opens up the interesting possibility of capturing native protein, cellular or nanomaterial configurations before radiation-induced effects have time to propagate through the structure, thus overcoming the limitation of radiation damage.

An important direction, especially for biological investigations, is the combination of light microscopy with electron microscopy. Radiation damage will probably prevent electron microscopy studies of processes in biological systems. However, these processes can be imaged with light microscopy, for example through phase contrast microscopy of the native cellular material or fluorescence microscopy of labelled proteins or other components in cells[98]. At a certain time of interest, the sample can be transferred to the TEM, STEM[4] or SEM for nanoscale investigation of the biological structure itself or of nanoparticles attached to the biological material. The type of sample and required resolution will determine the choice of electron microscopy modality. The temporal correlation of light and electron microscopy is typically several minutes, as the sample holder has to be transferred from one microscope to the other[49]. Integration of light microscopy with SEM[33], or fluorescence microscopy with TEM[99] or STEM, can allow temporal correlation within seconds.

Quantitative data acquisition is a key challenge for electron microscopy of liquids, in particular if we hope to use the technique to understand the fine details of static structures and to test models for dynamic processes. In conventional electron microscopy, a broad body of literature examines the effect of microscope parameters on image characteristics, and the effect of the electron beam on traditional solid samples and solid-state processes[8,9,71]. The same effort is now required for liquid samples. The equations above give guidance on the optimal parameters for imaging, but further experimental testing is required, especially regarding the improvements possible with aberration correction. Equally important is the need for a more rigorous understanding of beam–sample interactions for a variety of materials, so that guidelines can be developed for when and how imaging is likely to affect the results. Finally, for quantitative matching of data with models for dynamic events, such as particle growth and deposition, the liquid geometry and flow must be understood. Liquid movement, Brownian motion and diffusive phenomena in the restricted volume of an enclosed liquid cell form an interesting scientific topic of which understanding is required for developing quantitative models.

With these experimental advances, we anticipate that electron microscopy of liquid samples will play an important role in solving a broad set of scientific problems. Electron microscopy of biological samples in microfluidic devices may serve the pressing need for microscopy of cells and other biological systems and materials in their native liquid state with a resolution of a few nanometres — the dimension of proteins. Membrane receptors on intact cells can be studied in liquid[2,4,33] using labels with different size, shape and composition to tag different proteins. Labelling of intracellular proteins can be accomplished using emerging technologies[100,101]. The uptake of nanoparticles into the interior of cells can be studied with relevance for nanotoxicology[48,102,103]. Samples can be fixed after different time points to study processes involving multiple lipid and/or protein species[4]. Alternatively, using the correlative techniques discussed above, cells can be kept alive in a microfluidic chamber, monitored with fluorescence microscopy and imaged at certain times with electron microscopy[49]. With nanometre resolution and functionality similar to that of fluorescence microscopy, this approach will be significant for many fields of biological and biomedical research including virology, oncology, neuroscience and cell biology.

In materials science, electron microscopy of liquids is likely to play a central role in improving our understanding of reactions in energy materials, such as examination of failure modes of batteries during cycling[104,105], or to address new materials and microstructures for energy storage. Figure 4c, for example, shows the electrochemical formation of dendrites, a key failure mode for metal–air batteries that can be uniquely addressed by liquid cell electron microscopy[104]. Lithiation of anodes and formation of interfacial layers between electrolyte and electrodes are of particular relevance to commercial lithium-ion batteries, yet are difficult to study outside the liquid environment of the battery itself. Liquid cell electron microscopy is likely to make an impact in other areas as well, such as biomineralization with relevance for carbon dioxide sequestration, and in research on hydrated geological materials, such as clays, with applications in petroleum extraction and soil science. Complex nanoparticle arrays can be developed by directly visualizing self-assembly processes that are induced by external fields or by functionalization of the particles themselves. Controlled liquid mixing and application of heat, magnetic fields or other external stimuli will increase the range of processes that can be studied.

Electron microscopy of liquids has a long history, but a very interesting present. The upsurge in activity, the achievements of recent years and the broad range of areas in which the technique has been and could be applied suggest that numerous exciting developments can be expected in the future.

References

1. Ruska, E. Beitrag zur uebermikroskopischen Abbildungen bei hoeheren Drucken. *Kolloid Z.* **100,** 212–219 (1942).
   This paper describes the first *in situ* TEM — its principle of operation is still the basis of most modern *in situ* TEM systems.
2. Thiberge, S. *et al.* Scanning electron microscopy of cells and tissues under fully hydrated conditions. *Proc. Natl Acad. Sci. USA* **101,** 3346–3351 (2004).
   This paper made it clear that cells and tissue fully embedded in liquid can be imaged with a SEM with a resolution of several tens of nanometres.
3. Williamson, M. J., Tromp, R. M., Vereecken, P. M., Hull, R. & Ross, F. M. Dynamic microscopy of nanoscale cluster growth at the solid–liquid interface. *Nature Mater.* **2,** 532–536 (2003).
   This paper describes the first use of a silicon nitride liquid cell for measuring a growth process in the TEM, and the first combination of electrical biasing with liquid cell microscopy to control and quantify a growth process.
4. de Jonge, N., Peckys, D. B., Kremers, G. J. & Piston, D. W. Electron microscopy of whole cells in liquid with nanometer resolution. *Proc. Natl Acad. Sci. USA* **106,** 2159–2164 (2009).
   This paper is the first demonstration of the imaging of labelled proteins in whole eukaryotic cells in liquid with a resolution of several nanometres, using STEM.
5. Huang, J. Y. *et al. In situ* observation of the electrochemical lithiation of a single SnO_2 nanowire electrode. *Science* **330,** 1515–1520 (2010).
6. Zheng, H. *et al.* Observation of single colloidal platinum nanocrystal growth trajectories. *Science* **324,** 1309–1312 (2009).
   This paper is the first demonstration of the study of nanoparticle growth in liquid with nanometre resolution in TEM.
7. Ruska, E. The development of the electron microscope and of electron microscopy. *Nobel Lectures, Physics 1981–1990* (1986).
8. Reimer, L. & Kohl, H. *Transmission Electron Microscopy: Physics of Image Formation* (Springer, 2008).
9. Bozzola, J. J. & Russell, L. D. *Electron Microscopy* (Jones and Bartlett, 1992).
10. von Ardenne, M. Ueber eun 200 kV-Universal-Elektronenmikroskop mit Objektabschattungsvorrichtung. *Z. Phys.* **117,** 657–688 (1941).
11. Donnelly, S. E. *et al.* Ordering in a fluid inert gas confined by flat surfaces. *Science* **296,** 507–510 (2002).
12. Parsons, D. F., Matricardi, V. R., Moretz, R. C. & Turner, J. N. Electron microscopy and diffraction of wet unstained and unfixed biological objects. *Adv. Biol. Med. Phys.* **15,** 161–270 (1974).
13. Helveg, S. *et al.* Atomic-scale imaging of carbon nanofibre growth. *Nature* **427,** 426–429 (2004).
14. Dai, L. L., Sharma, R. & Wu, C. Y. Self-assembled structure of nanoparticles at a liquid–liquid interface. *Langmuir* **21,** 2641–2643 (2005).
15. Danilatos, G. D. & Robinson, V. N. E. Principles of scanning electron microscopy at high specimen pressures. *Scanning* **18,** 75–78 (1979).
16. Stokes, D. J. Recent advances in electron imaging, image interpretation and applications: environmental scanning electron microscopy. *Phil. Trans. R. Soc. Lond. A* **361,** 2771–2787 (2003).

© 2011 Macmillan Publishers Limited. All rights reserved

17. Stokes, D. L. *Principles and Practice of Variable Pressure/Environmental Scanning Electron Microscopy (VP-SEM)* (Wiley, 2008).
18. Abrams, I. M. & McBain, J. W. A closed cell for electron microscopy. *J Appl. Phys.* **15,** 607–609 (1944).
19. Daulton, T. L., Little, B. J., Lowe, K. & Jones-Meehan, J. *In situ* environmental cell–transmission electron microscopy study of microbial reduction of chromium(VI) using electron energy loss spectroscopy. *Microsc. Microanal.* **7,** 470–485 (2001).
20. Nishijima, K., Yamasaki, J., Orihara, H. & Tanaka, N. Development of microcapsules for electron microscopy and their application to dynamical observation of liquid crystals in transmission electron microscopy. *Nanotechnology* **15,** S329–S332 (2004).
21. Mohanty, N., Fahrenholtz, M., Nagaraja, A., Boyle, D. & Berry, V. Impermeable graphenic encasement of bacteria. *Nano Lett.* **11,** 1270–1275 (2011).
22. Grogan, J. M. & Bau, H. H. The nanoaquarium: a platform for *in situ* transmission electron microscopy in liquid media. *J. Microelectromech. Syst.* **19,** 885–894 (2010).
23. Franks, R. *et al.* A study of nanomaterial dispersion in solution by wet-cell transmission electron microscopy. *J. Nanosci. Nanotechnol.* **8,** 4404–4407 (2008).
24. Liu, K. L. *et al.* Novel microchip for *in situ* TEM imaging of living organisms and bio-reactions in aqueous conditions. *Lab Chip* **8,** 1915–1921 (2008).
25. Ring, E. A. & de Jonge, N. Microfluidic system for transmission electron microscopy. *Microsc. Microanal.* **16,** 622–629 (2010).
26. de Jonge, N., Poirier-Demers, N., Demers, H., Peckys, D. B. & Drouin, D. Nanometer-resolution electron microscopy through micrometers-thick water layers. *Ultramicroscopy* **110,** 1114–1119 (2010).
27. Peckys, D. B., Veith, G. M., Joy, D. C. & de Jonge, N. Nanoscale imaging of whole cells using a liquid enclosure and a scanning transmission electron microscope. *PLoS One* **4**, e8214 (2009).
28. Creemer, J. F. *et al.* Atomic-scale electron microscopy at ambient pressure. *Ultramicroscopy* **108,** 993–998 (2008).
This paper describes advances in high-pressure cells for the TEM that combine enhanced functionality with the ability to image at atomic resolution.
29. Creemer, J. F. *et al.* A MEMS reactor for atomic-scale microscopy of nanomaterials under industrially relevant conditions. *J. Microelectromech. Syst.* **19,** 254–264 (2010).
30. Kawasaki, T., Ueda, K., Ichihashi, M. & Tanji, T. Improvement of windowed type environmental-cell transmission electron microscope for *in situ* observation of gas-solid interactions. *Rev. Sci. Instr.* **80,** 113701–113705 (2009).
31. Klein, K. L., Anderson, I. M. & de Jonge, N. Transmission electron microscopy with a liquid flow cell. *J. Microsc.* **242,** 117–123 (2011).
32. Zheng, H., Claridge, S. A., Minor, A. M., Alivisatos, A. P. & Dahmen, U. Nanocrystal diffusion in a liquid thin film observed by *in situ* transmission electron microscopy. *Nano Lett.* **9,** 2460–2465 (2009).
33. Nishiyama, H. *et al.* Atmospheric scanning electron microscope observes cells and tissues in open medium through silicon nitride film. *J. Struct. Biol.* **169,** 438–449 (2010).
34. Inami, W., Nakajima, K., Miyakawa, A. & Kawata, Y. Electron beam excitation assisted optical microscope with ultra-high resolution. *Opt. Express* **18,** 12897–12902 (2010).
35. Evans, J. E., Jungjohann, K. L., Browning, N. D. & Arslan, I. Controlled growth of nanoparticles from solution with *in situ* liquid transmission electron microscopy. *Nano Lett.* **11,** 2809–2813 (2011).
36. Sali, A., Glaeser, R., Earnest, T. & Baumeister, W. From words to literature in structural proteomics. *Nature* **422,** 216–225 (2003).
37. Stahlberg, H. & Walz, T. Molecular electron microscopy: state of the art and current challenges. *ACS Chem. Biol.* **3,** 268–281 (2008).
38. Pierson, J., Sani, M., Tomova, C., Godsave, S. & Peters, P. J. Toward visualization of nanomachines in their native cellular environment. *Histochem. Cell. Biol.* **132,** 253–262 (2009).
39. Kirk, S. E., Skepper, J. N. & Donald, A. M. Application of environmental scanning electron microscopy to determine biological surface structure. *J. Microsc.* **233,** 205–224 (2009).
40. Collins, S. P. *et al.* Advantages of environmental scanning electron microscopy in studies of microorganisms. *Microsc. Res. Techniq.* **25,** 398–405 (1993).
41. Bogner, A., Thollet, G., Basset, D., Jouneau, P. H. & Gauthier, C. Wet STEM: A new development in environmental SEM for imaging nano-objects included in a liquid phase. *Ultramicroscopy* **104,** 290–301 (2005).
42. Xiao, Y., Patolsky, F., Katz, E., Hainfeld, J. F. & Willner, I. 'Plugging into enzymes': nanowiring of redox enzymes by a gold nanoparticle. *Science* **299,** 1877–1881 (2003).
43. Barshack, I. *et al.* A novel method for 'wet' SEM. *Ultrastruct. Pathol.* **28,** 29–31 (2004).
44. Melo, R. C., Sabban, A. & Weller, P. F. Leukocyte lipid bodies: inflammation-related organelles are rapidly detected by wet scanning electron microscopy. *J. Lipid. Res.* **47,** 2589–2594 (2006).
45. Sugi, H. *et al.* Dynamic electron microscopy of ATP-induced myosin head movement in living muscle filaments. *Proc. Natl Acad. Sci. USA* **94,** 4378–4392 (1997).
46. Matricardi, V. R., Moretz, R. C. & Parsons, D. F. Electron diffraction of wet proteins: catalase. *Science* **177,** 268–270 (1972).
47. Lippincott-Schwartz, J. & Manley, S. Putting super-resolution fluorescence microscopy to work. *Nature Methods* **6,** 21–23 (2009).
48. Peckys, D. B. & de Jonge, N. Visualization of gold nanoparticle uptake in living cells with liquid scanning transmission electron microscopy. *Nano Lett.* **11,** 1733–1738 (2011).
49. Peckys, D. B., Mazur, P., Gould, K. L. & de Jonge, N. Fully hydrated yeast cells imaged with electron microscopy. *Biophys. J.* **100,** 2522–2529 (2011).
50. Murai, T. *et al.* Low cholesterol triggers membrane microdomain-dependent CD44 shedding and suppresses tumor cell migration. *J. Biol. Chem.* **286,** 1999–2007 (2011).
51. Dukes, M. J., Peckys, D. B. & de Jonge, N. Correlative fluorescence microscopy and scanning transmission electron microscopy of quantum-dot-labeled proteins in whole cells in liquid. *ACS Nano* **4,** 4110–4116 (2010).
52. Radisic, A., Vereecken, P. M., Hannon, J. B., Searson, P. C. & Ross, F. M. Quantifying electrochemical nucleation and growth of nanoscale clusters using real-time kinetic data. *Nano Lett.* **6,** 238–242 (2006).
53. Scharifker, B. R. & Hills, G. J. Theoretical and experimental studies of multiple nucleation. *Electrochim. Acta* **28,** 879–889 (1983).
54. Radisic, A., Ross, F. M. & Searson, P. C. *In situ* study of the growth kinetics of individual island electrodeposition of copper. *J. Phys. Chem. B* **110,** 7862–7868 (2006).
55. Radisic, A., Vereecken, P. M., Searson, P. C. & Ross, F. M. The morphology and nucleation kinetics of copper islands during electrodeposition. *Surf. Sci.* **600,** 1817–1826 (2006).
56. Wise, M. E., Biskos, G., Martin, S. T., Russell, L. M. & Buseck, P. R. Phase transitions of single salt particles studied using a transmission electron microscope with an environmental cell. *Aerosol. Sci. Tech.* **39,** 849–856 (2005).
57. Gai, P. L. Development of wet environmental TEM (wet-ETEM) for *in situ* studies of liquid-catalyst reactions on the nanoscale. *Microsc. Microanal.* **8,** 21–28 (2002).
The first observation by TEM of an industrially important liquid-phase catalytic reaction.
58. Gai, P. L. & Harmer, M. A. Surface atomic defect structures and growth of Au nanorods. *Nano Lett.* **2,** 771–774 (2002).
59. Gabrisch, H., Kjeldgaard, L., Johnson, E. & Dahmen, U. Equilibrium shape and interface roughening of small liquid Pb inclusions in solid Al. *Acta Mater.* **49,** 4259–4269 (2001).
60. Ross, F. M., Tersoff, J. & Reuter, M. C. Sawtooth faceting in silicon nanowires. *Phys. Rev. Lett.* **95,** 146104 (2005).
61. Eswaramoorthy, S. K., Howe, J. M. & Muralidharan, G. *In situ* determination of the nanoscale chemistry and behavior of solid-liquid systems. *Science* **318,** 1437–1440 (2007).
62. Lee, J. G. & Mori, H. *In situ* observation of alloy phase formation in nanometre-sized particles in the Sn–Bi system. *Philos. Mag.* **84,** 2675–2686 (2004).
63. Howe, J. M. & Saka, H. *In situ* transmission electron microscopy studies of the solid–liquid interface. *MRS Bull.* **29,** 951–957 (2004).
64. Kuwabata, S., Kongkanand, A., Oyamatsu, D. & Torimoto, T. Observation of ionic liquid by scanning electron microscope. *Chem. Lett.* **35,** 600–601 (2006).
65. Roy, P., Lynch, R. & Schmuki, P. Electron beam induced *in vacuo* Ag deposition on TiO_2 from ionic liquids. *Electrochem. Comm.* **11,** 1567–1570 (2009).
66. Joy, D. C. & Joy, C. S. Scanning electron microscope imaging in liquids — some data on electron interactions in water. *J. Microsc.* **221,** 84–99 (2005).
67. Hyun, J. K., Ercius, P. & Muller, D. A. Beam spreading and spatial resolution in thick organic specimens. *Ultramicroscopy* **109,** 1–7 (2008).
68. Loos, J. *et al.* Electron tomography on micrometer-thick specimens with nanometer resolution. *Nano Lett.* **9,** 1704–1708 (2009).
69. Demers, H., Poirier-Demers, N., Drouin, D. & de Jonge, N. Simulating STEM imaging of nanoparticles in micrometers-thick substrates. *Microsc. Microanal.* **16,** 795–804 (2010).
70. Sousa, A. A., Hohmann-Marriott, M. F., Zhang, G. & Leapman, R. D. Monte Carlo electron-trajectory simulations in bright-field and dark-field STEM: implications for tomography of thick biological sections. *Ultramicroscopy* **109,** 213–221 (2009).
71. Spence, J. C. H. *High-Resolution Electron Microscopy* (Oxford Univ. Press, 2003).
72. Hohmann-Marriott, M. F. *et al.* Nanoscale 3D cellular imaging by axial scanning transmission electron tomography. *Nature Methods* **6,** 729–731 (2009).

© 2011 Macmillan Publishers Limited. All rights reserved

73. Aoyama, K., Takagi, T., Hirase, A. & Miyazawa, A. STEM tomography for thick biological specimens. *Ultramicroscopy* **109,** 70–80 (2008).
74. Crewe, A. V., Wall, J. & Langmore, J. Visibility of single atoms. *Science* **168,** 1338–1340 (1970).
75. Krivanek, O. L. *et al.* Atom-by-atom structural and chemical analysis by annular dark-field electron microscopy. *Nature* **464,** 571–574 (2010).
76. Goldstein, J. I. in *Introduction to Analytical Electron Microscopy* (eds Hren, J. J., Goldstein, J. I. & Joy, D. C.) 83–120 (Plenum Press, 1979).
77. Thiberge, S., Zik, O. & Moses, E. An apparatus for imaging liquids, cells, and other wet samples in the scanning electron microscopy. *Rev. Sci. Instrum.* **75,** 2280–2289 (2004).
78. Fenter, P., Lee, S. S., Zhang, Z. & Sturchio, N. C. *In situ* imaging of orthoclase-aqueous solution interfaces with X-ray reflection interface microscopy. *J. Appl. Phys.* (in the press).
79. Garrett, B. C. *et al.* Role of water in electron-initiated processes and radical chemistry: issues and scientific advances. *Chem. Rev.* **105,** 355–390 (2005).
80. Donev, E. U., Schardein, G., Wright, J. C. & Hastings, J. T. Substrate effects on the electron-beam-induced deposition of platinum from a liquid precursor. *Nanoscale* **3,** 2709–2717 (2011).
81. Hui, S. W. & Parsons, D. F. Electron diffraction of wet biological membranes. *Science* **184,** 77–78 (1974).
82. Kenworthy, A. K. *et al.* Dynamics of putative raft-associated proteins at the cell surface. *J. Cell Biol.* **165,** 735–746 (2004).
83. Holmqvist, P., Dhont, J. K. G. & Lang, P. R. Anisotropy of Brownian motion caused only by hydrodynamic interaction with a wall. *Phys. Rev. E* **74,** 021402 (2006).
84. Pawley, J. B. *Handbook of Biological Confocal Microscopy* (Springer, 1995).
85. Hell, S. W. Far-field optical nanoscopy. *Science* **316,** 1153–1158 (2007). **This paper reviews several light microscopy approaches to break the diffraction barrier**.
86. Betzig, E., Trautman, J. K., Harris, T. D., Weiner, J. S. & Kostelak, R. L. Breaking the diffraction barrier: optical microscopy on a nanometric scale. *Science* **251,** 1468–1470 (1991).
87. Chao, W., Harteneck, B. D., Liddle, J. A., Anderson, E. H. & Attwood, D. T. Soft X-ray microscopy at a spatial resolution better than 15 nm. *Nature* **435,** 1210–1213 (2005).
88. Larabell, C. A. & Nugent, K. A. Imaging cellular architecture with X-rays. *Curr. Opin. Struct. Biol.* **20,** 623–631 (2010).
89. Muller, D. J., Helenius, J., Alsteens, D. & Dufrene, Y. F. Force probing surfaces of living cells to molecular resolution. *Nature Chem. Biol.* **5,** 383–390 (2009).
90. Allison, D. P., Mortensen, N. P., Sullivan, C. J. & Doktycz, M. J. Atomic force microscopy of biological samples. *Nanomed. Nanobiotechnol.* **2,** 618–634 (2010).
91. Fleming, A. J., Kenton, B. J. & Leang, K. K. Bridging the gap between conventional and video-speed scanning probe microscopes. *Ultramicroscopy* **110,** 1205–1214 (2010).
92. Sulchek, T. *et al.* High-speed atomic force microscopy in liquid. *Rev. Sci. Instrum.* **71,** 2097–2099 (2000).
93. Langmore, J. P. & Smith, M. F. Quantitative energy-filtered electron microscopy of biological molecules in ice. *Ultramicroscopy* **46,** 349–373 (1992).
94. Haider, M., Hartel, P., Muller, H., Uhlemann, S. & Zach, J. Current and future aberration correctors for the improvement of resolution in electron microscopy. *Phil. Trans. R. Soc. A* **367,** 3665–3682 (2009).
95. Flannigan, D. J., Barwick, B. & Zewail, A. H. Biological imaging with 4D ultrafast electron microscopy. *Proc. Natl Acad. Sci. USA* **107,** 9933–9937 (2010).
96. Campbell, G. H., LaGrange, T., Kim, J. S., Reed, B. W. & Browning, N. D. Quantifying transient states in materials with the dynamic transmission electron microscope. *J. Electron Microsc.* **59** (suppl. 1), S67–S74 (2010).
97. Kruit, P. & Jansen, G. H. in *Handbook of Charged Particle Optics* (ed. Orloff, J.) 275–318 (CRC Press, 1997).
98. Lippincott-Schwartz, J., Snapp, E. & Kenworthy, A. Studying protein dynamics in living cells. *Nature Rev. Mol. Cell Biol.* **2,** 444–456 (2001).
99. Agronskaia, A. V. *et al.* Integrated fluorescence and transmission electron microscopy. *J. Struct. Biol.* **164,** 183–189 (2008).
100. Shu, X. *et al.* A genetically encoded tag for correlated light and electron microscopy of intact cells, tissues, and organisms. *PLoS Biol.* **9,** e1001041 (2011).
101. Chou, L. Y., Ming, K. & Chan, W. C. Strategies for the intracellular delivery of nanoparticles. *Chem. Soc. Rev.* **40,** 233–245 (2011).
102. Tkachenko, A. G. *et al.* Cellular trajectories of peptide-modified gold particle complexes: comparison of nuclear localization signals and peptide transduction domains. *Bioconjugate Chem.* **15,** 482–490 (2004).
103. Tantra, R. & Knight, A. Cellular uptake and intracellular fate of engineered nanoparticles: A review on the application of imaging techniques. *Nanotoxicology* **5,** 381–392 (2010).
104. Ross, F. M. Electrochemical nucleation, growth and dendrite formation in liquid cell TEM. *Microsc. Microanal.* **16,** S326–S327 (2010).
105. Wang, C. M. *et al. In situ* transmission electron microscopy and spectroscopy studies of interfaces in Li-ion batteries: challenges and opportunities. *J. Mater. Res.* **25,** 1541–1547 (2010).

Acknowledgements

This work was supported by Vanderbilt University School of Medicine and by IBM.

Additional information

The authors declare no competing financial interests.

© 2011 Macmillan Publishers Limited. All rights reserved